

RESEARCH ARTICLE

Adaptive greedy algorithms based on parameter-domain decomposition and reconstruction for the reduced basis method

Jiahua Jiang¹ | Yanlai Chen^{*2}

¹Department of Mathematics, Virginia Tech University, VA, U.S.A.

Email: jiahua@vt.edu

²Department of Mathematics, University of Massachusetts Dartmouth, MA, U.S.A.

Email: Yanlai.Chen@umassd.edu

Correspondence

*Corresponding author.

Summary

The reduced basis method (RBM) empowers repeated and rapid evaluation of parametrized partial differential equations through an offline-online decomposition, a.k.a. a learning-execution process. A key feature of the method is a greedy algorithm repeatedly scanning the training set, a fine discretization of the parameter domain, to identify the next dimension of the parameter-induced solution manifold along which we expand the surrogate solution space. Although successfully applied to problems with fairly high parametric dimensions, the challenge is that this scanning cost dominates the offline cost due to it being proportional to the cardinality of the training set which is exponential with respect to the parameter dimension. In this work, we review three recent attempts in effectively delaying this curse of dimensionality, and propose two new hybrid strategies through successive refinement and multilevel maximization of the error estimate over the training set. All five offline-enhanced methods and the original greedy algorithm are tested and compared on two types of problems: the thermal block problem and the geometrically parameterized Helmholtz problem.

KEYWORDS:

Reduced basis method, Greedy algorithm

1 | INTRODUCTION

The reduced basis method (RBM)^{1,2} has proved to be a viable option for the purpose of designing fast numerical algorithms for parametrized systems. The parameters (denoted by $\boldsymbol{\mu}$ throughout this paper) may include boundary conditions, material properties, amount of uncertainty, geometric configurations, source properties etc. To describe a realistic system, practitioners often resort to a large number of parameters making the the generation of a reduced model computationally challenging.

The critical ingredient enabling RBM to attain orders of magnitude gain in marginal (i.e. per parameter instance) computation time, is an offline-online decomposition process where the basis selection (i.e. surrogate solution space building) is performed offline by a greedy algorithm, see e.g.^{3,4,5,6} for details. The ultimate goal is that the complexity of the reduced solver, presumably to be called for an overwhelming number of times or even in a realtime fashion, is independent of the degrees of freedom (denoted by \mathcal{N} throughout this paper) of the full order model (FOM, a.k.a. “truth” in the RB literature) approximation.

The construction of the reduced basis space relies on a greedy scheme that keeps track of an efficiently-computable error estimator/indicator, denoted by $\Delta_n(\boldsymbol{\mu})$, indicating the discrepancy between the dimension- n surrogate solution (RB solution) and the FOM solution. This greedy procedure starts by selecting the first parameter $\boldsymbol{\mu}^1$ randomly from the training set (i.e. a discretized version of the parameter domain) and obtaining its corresponding truth approximation $u^{\mathcal{N}}(\boldsymbol{\mu}^1)$. We then have a one-dimensional RB space $W_1 = \{u^{\mathcal{N}}(\boldsymbol{\mu}^1)\}$. Next, the scheme obtains an RB approximation $u_1^{\mathcal{N}}(\boldsymbol{\mu})$ for each parameter in the training

set together with $\Delta_1(\boldsymbol{\mu})$. The greedy choice for the $(n + 1)$ th parameter ($n = 1, 2, \dots$) is made and the RB space augmented by

$$\boldsymbol{\mu}^{n+1} = \underset{\boldsymbol{\mu} \in \Xi_{\text{train}}}{\operatorname{argmax}} \Delta_n(\boldsymbol{\mu}), \quad W_{n+1} = W_n \oplus \{u^N(\boldsymbol{\mu}^{n+1})\}. \quad (1)$$

The other parts of the offline process are devoted to the necessary preparations for the online reduced solver, a variational (i.e. Galerkin or Petrov-Galerkin) projection^{7,8,9} into the surrogate space, or a representation of the solution at strategically chosen points in the physical domain^{10,11}. The greedy procedure (1) implies that the offline cost is proportional to the cardinality of the training set Ξ_{train} . It is essential for this training set to be fine enough so that we are not missing critical phenomena not represented by Ξ_{train} . In particular, its cardinality is exponential with respect to the parameter dimension. As a consequence, the ‘‘break-even’’ number of simulations for the parametric system (i.e. minimum number of simulations that makes the offline preparation stage worthwhile) is exponential with respect to the parameter dimension as well, severely diminishing the attractiveness of RBM.

The need of delaying this curse of dimensionality motivates numerous recent attempts in designing offline-enhancement strategies for systems with high-dimensional parameter domain. Indeed, the authors of¹² propose a static decomposition of the given parameter training set Ξ_{train} *a priori* into a sequence of subsets that increase geometrically in size, and then perform the classical greedy algorithm on each of them sequentially. The idea is that scanning smaller sets will quickly result in a reduced solver capable of resolving a significant part of the larger sets making them more affordable for scanning. Authors of¹³ take a different route. They fix the cardinality of an active training set that is much smaller than the full training set. After each greedy step, the active training set is pruned (with the parameters whose error estimates are below the tolerance) and replenished to the original cardinality with random selections from the full training set. Finally,¹⁴ promotes to recycle the information afforded by the error estimates $\{\Delta_n(\boldsymbol{\mu})\}$ and to adaptively construct a surrogate training set. The adaptive nature of the construction which, moreover, is informed by the error estimate makes it potentially more effective than the approach of¹². There have been other techniques in the literature to alleviate the RB offline cost such as the parameter domain adaptivity^{15,16}, greedy sampling acceleration through nonlinear optimization^{17,18}, and local reduced basis method^{19,20,21,22}, etc.

In this paper, we focus on the three approaches of^{12,13,14} that are similar in nature. We review the essence of each algorithm, compare them, and more importantly, propose two new hybrid strategies through successive refinement and multilevel maximization of $\{\Delta_n(\boldsymbol{\mu})\}$ over the training set. By testing all these five strategies and the classical greedy, we demonstrate that the two new hybrids outperform others some of which may even fail for a more challenging geometrically parameterized Helmholtz problem.

The paper is organized as follows. In Section 2, we review the three existing offline enhancement approaches mentioned above. In Section 3, the two new hybrid approaches are introduced. Numerical results for two test problems to demonstrate the accuracy and efficiency of these offline improvement methods are shown in Section 4. Finally, concluding remarks are drawn in Section 5.

2 | BACKGROUND

In this section, we briefly review the classical reduced basis method and the three offline enhancement strategies. This also serves as a background and motivation for the subsequent discussion of our newly proposed multi-level greedy techniques leading to more efficient reduced basis methods. Table 1 outlines our notations.

2.1 | Reduced Basis Methods

We first provide an overview of the essential ingredients of RBM in its classical form. For more details see e.g.^{1,2,3,4}. Indeed, given $\boldsymbol{\mu} \in \mathcal{D}$, the goal is to evaluate a certain output of interest

$$s(\boldsymbol{\mu}) = \ell(u(\boldsymbol{\mu}); \boldsymbol{\mu}), \quad (2)$$

where the function $u(\boldsymbol{\mu}) \in X$ satisfies

$$a(u(\boldsymbol{\mu}), v; \boldsymbol{\mu}) = f(v; \boldsymbol{\mu}), \quad v \in X, \quad (3)$$

which is a parametrized partial differential equation (pPDE) written in a weak form with $\boldsymbol{\mu} \in \mathcal{D}$ being the (possibly multi-dimension) parameter. Here $X = X(\Omega)$ is a Hilbert space satisfying, e.g., $H_0^1(\Omega) \subset X(\Omega) \subset H^1(\Omega)$. We denote by $(\cdot, \cdot)_X$ the inner product associated with the space X , whose induced norm $\|\cdot\|_X = \sqrt{(\cdot, \cdot)_X}$ is equivalent to the usual $H^1(\Omega)$ norm. We

$\boldsymbol{\mu}$	Parameter in $\mathcal{D} \subseteq \mathbb{R}^p$
$u(\boldsymbol{\mu})$	Function-valued solution of a parameterized PDE
\mathcal{N}	Degrees of freedom (DoF) in PDE "truth" solver
$u^{\mathcal{N}}(\boldsymbol{\mu})$	Truth solution (finite-dimensional)
N	Number of reduced basis snapshots, $N \ll \mathcal{N}$
N_{max}	Terminal number of reduced bases
$\boldsymbol{\mu}^j$	"Snapshot" parameter values, $j = 1, \dots, N$
$X_N^{\mathcal{N}}$	Span of $u^{\mathcal{N}}(\boldsymbol{\mu}^k)$ for $k = 1, \dots, N$
$u_N^{\mathcal{N}}(\boldsymbol{\mu})$	Reduced basis solution, $u_N^{\mathcal{N}} \in X_N^{\mathcal{N}}$
$e_N(\boldsymbol{\mu})$	Reduced basis solution error, equals $u^{\mathcal{N}}(\boldsymbol{\mu}) - u_N^{\mathcal{N}}(\boldsymbol{\mu})$
Ξ_{train}	Parameter training set, a finite subset of \mathcal{D}
n_{train}	Size of Ξ_{train}
$\Delta_N(\boldsymbol{\mu})$	Error estimate (upper bound) for $\ e_N(\boldsymbol{\mu})\ $
ϵ_{tol}	Error estimate stopping tolerance in greedy sweep
A priori training set decomposition	
\mathcal{J}	Number of sample sets
$\Xi_{train,j}$	The j -th sample set
$\Delta_{N,j}(\boldsymbol{\mu})$	A posteriori error estimate with N reduced bases at j -th sample set
Adaptive enriching	
Ξ	Sample parameters of fixed cardinality ($\ll n_{train}$)
M_{sample}	Size of the active training set Ξ , much smaller than n_{train}
Adaptive construction of surrogate training sets	
ℓ	Number of "outer" loops in the offline enhancement procedure, Algorithm 4
E_ℓ	The largest error estimator at the beginning of outer loop ℓ
Ξ_{sur}	Surrogate Training Set (STS), a subset of Ξ_{train}
K_{damp}	A constant integer controlling the damping ratio of the error estimate when examining the STS
C_M	A constant integer adjusting the size of surrogate training set

TABLE 1 Notation used throughout this article.

typically assume that $a(\cdot, \cdot; \boldsymbol{\mu}) : X \times X \rightarrow \mathbb{R}$ is continuous and coercive over X uniformly in $\boldsymbol{\mu} \in \mathcal{D}$, that is,

$$\gamma(\boldsymbol{\mu}) := \sup_{w \in X} \sup_{v \in X} \frac{a(w, v; \boldsymbol{\mu})}{\|w\|_X \|v\|_X} < \infty, \quad \forall \boldsymbol{\mu} \in \mathcal{D}, \quad (4a)$$

$$\alpha(\boldsymbol{\mu}) := \inf_{w \in X} \frac{|a(w, w; \boldsymbol{\mu})|}{\|w\|_X^2} \geq \alpha_0 > 0, \quad \forall \boldsymbol{\mu} \in \mathcal{D}. \quad (4b)$$

$f(\cdot)$ and $\ell(\cdot)$ are linear continuous functionals over X . We assume that there is a finite-dimensional discretization for the model problem (3): The solution space X is discretized by an \mathcal{N} -dimensional space $X^{\mathcal{N}}$ (i.e., $\dim(X^{\mathcal{N}}) = \mathcal{N}$) and (2) and (3) are discretized as

$$\begin{cases} \text{For } \boldsymbol{\mu} \in \mathcal{D}, \text{ solve} \\ s^{\mathcal{N}} = \ell(u^{\mathcal{N}}(\boldsymbol{\mu}); \boldsymbol{\mu}) \text{ where } u^{\mathcal{N}}(\boldsymbol{\mu}) \in X^{\mathcal{N}} \text{ satisfies} \\ a(u^{\mathcal{N}}, v; \boldsymbol{\mu}) = f(v; \boldsymbol{\mu}) \quad \forall v \in X^{\mathcal{N}}. \end{cases} \quad (5)$$

The relevant quantities such as the coercivity constant (4b) are defined according to the discretization,

$$\alpha^{\mathcal{N}}(\boldsymbol{\mu}) = \inf_{w \in X^{\mathcal{N}}} \frac{a(w, w; \boldsymbol{\mu})}{\|w\|_X^2} \geq \alpha(\boldsymbol{\mu}) \geq \alpha_0, \quad \forall \boldsymbol{\mu} \in \mathcal{D}.$$

In the RBM literature, any quantity associated to \mathcal{N} is called a "truth" (FOM). E.g., $u^{\mathcal{N}}$ is called the "truth solution", (5) "truth solver". \mathcal{N} is typically very large so that resolving the FOM gives highly accurate approximations for all $\boldsymbol{\mu} \in \mathcal{D}$.

For a training set $\Xi_{\text{train}} \subset \mathcal{D}$ which consists of a fine discretization of \mathcal{D} of finite cardinality and a collection of N parameters $\mathcal{S}_N = \{\boldsymbol{\mu}^1, \dots, \boldsymbol{\mu}^N\} \subset \Xi_{\text{train}}$, we define the reduced basis space as

$$X_N^{\mathcal{N}} := \text{span}\{u^{\mathcal{N}}(\boldsymbol{\mu}^n), 1 \leq n \leq N\}. \quad (6)$$

The reduced basis approximation is now defined as: Given $\boldsymbol{\mu} \in \mathcal{D}$, seek a surrogate RB solution $u_N^{\mathcal{N}}(\boldsymbol{\mu})$ by solving the following reduced system

$$\begin{cases} \text{For } \boldsymbol{\mu} \in \mathcal{D}, \text{ evaluate} \\ s_N^{\mathcal{N}} = \ell(u_N^{\mathcal{N}}(\boldsymbol{\mu}); \boldsymbol{\mu}) \text{ s.t. } u_N^{\mathcal{N}}(\boldsymbol{\mu}) \in X_N^{\mathcal{N}} \subset X^{\mathcal{N}} \text{ satisfies} \\ a(u_N^{\mathcal{N}}, v; \boldsymbol{\mu}) = f(v) \quad \forall v \in X_N^{\mathcal{N}}. \end{cases} \quad (7)$$

(7) is called the reduced solver, i.e. Reduced Order Model (ROM). The typical multiple orders of magnitude speedup of RBM manifests from that the assembly of ROM is independent of \mathcal{N} , which crucially relies on the affine assumption of the parameter dependent problem (3), such as,

$$a(w, v; \boldsymbol{\mu}) = \sum_{q=1}^{Q_a} \Theta_a^q(\boldsymbol{\mu}) a^q(w, v), \quad \text{and} \quad f(v; \boldsymbol{\mu}) = \sum_{q=1}^{Q_f} \Theta_f^q(\boldsymbol{\mu}) f^q(v). \quad (8)$$

Here Θ_a^q, Θ_f^q are $\boldsymbol{\mu}$ -dependent functions, and a^q, f^q are $\boldsymbol{\mu}$ -independent forms. With Galerkin procedure in (7), the RB solution $u_N^{\mathcal{N}}$ for any parameter $\boldsymbol{\mu} \in \mathcal{D}$ can be represented as

$$u_N^{\mathcal{N}}(\boldsymbol{\mu}) = \sum_{i=1}^N u_{Ni}^{\mathcal{N}}(\boldsymbol{\mu}) u^{\mathcal{N}}(\boldsymbol{\mu}^i), \quad (9)$$

where $\{u_{Ni}^{\mathcal{N}}(\boldsymbol{\mu})\}_{i=1}^N$ are the RB coefficients obtained by solving (7)¹. With the affine hypothesis (8), we can apply an offline-online decomposition to enable fast resolution of the ROM (7). In the offline stage, we replace the reduced basis solution in (7) by (9) and choose $v = u^{\mathcal{N}}(\boldsymbol{\mu}^j), 1 \leq j \leq N$ as our test functions. Then we obtain the RB ‘‘stiffness’’ equations

$$\sum_{i=1}^N a(u^{\mathcal{N}}(\boldsymbol{\mu}^i), u^{\mathcal{N}}(\boldsymbol{\mu}^j); \boldsymbol{\mu}) u_{Ni}^{\mathcal{N}}(\boldsymbol{\mu}) = f(u^{\mathcal{N}}(\boldsymbol{\mu}^j); \boldsymbol{\mu}) \quad 1 \leq j \leq N. \quad (10)$$

Toward a fast construction of the stiff matrix, we plug (9) into (10) to obtain,

$$\sum_{q=1}^{Q_a} \sum_{i=1}^N \Theta_a^q(\boldsymbol{\mu}) a^q(u^{\mathcal{N}}(\boldsymbol{\mu}^i), u^{\mathcal{N}}(\boldsymbol{\mu}^j)) u_{Ni}^{\mathcal{N}}(\boldsymbol{\mu}) = \sum_{q=1}^{Q_f} \Theta_f^q(\boldsymbol{\mu}) f^q(u^{\mathcal{N}}(\boldsymbol{\mu}^j)) \quad 1 \leq j \leq N. \quad (11)$$

and precompute $a^q(u^{\mathcal{N}}(\boldsymbol{\mu}^i), u^{\mathcal{N}}(\boldsymbol{\mu}^j))$ and $f^q(u^{\mathcal{N}}(\boldsymbol{\mu}^j))$, which are relatively expensive but only done once. In the online stage, we construct the matrices and vectors in the reduced system (7) and solve the resulting reduced basis problem. We remark that when assumption (8) is violated, we turn to Empirical Interpolation Method (EIM)^{23,24,25} to approximate the non-affine operators by affine ones. This is the case for our second test problem in Section 4.2.

Leading to the key error estimator $\Delta_N(\boldsymbol{\mu})$, we define the error $e_N(\boldsymbol{\mu}) := u^{\mathcal{N}}(\boldsymbol{\mu}) - u_N^{\mathcal{N}}(\boldsymbol{\mu}) \in X^{\mathcal{N}}$. The linearity of $a(\cdot, \cdot; \boldsymbol{\mu})$ yields the following error equation:

$$a(e_N(\boldsymbol{\mu}), v; \boldsymbol{\mu}) = r_N(v; \boldsymbol{\mu}) \quad \forall v \in X^{\mathcal{N}}, \quad (12)$$

where the residual $r_N(\cdot; \boldsymbol{\mu}) \in (X^{\mathcal{N}})'$ (the dual of $X^{\mathcal{N}}$) operated on $v \in X^{\mathcal{N}}$ is defined as $f(v; \boldsymbol{\mu}) - a(u_N^{\mathcal{N}}(\boldsymbol{\mu}), v; \boldsymbol{\mu})$. We define the *a posteriori* error estimator for the solution, which is a rigorous bound for the error, as

$$\Delta_N(\boldsymbol{\mu}) = \frac{\|r_N(\cdot; \boldsymbol{\mu})\|_{(X^{\mathcal{N}})'}}{\alpha_{LB}^{\mathcal{N}}(\boldsymbol{\mu})} \geq \|e_N(\boldsymbol{\mu})\|_{(X^{\mathcal{N}})}, \quad (13)$$

where $\alpha_{LB}^{\mathcal{N}}(\boldsymbol{\mu})$ is a lower bound of the coercivity constant $\alpha^{\mathcal{N}}(\boldsymbol{\mu})$. The otherwise expensive evaluation of $\alpha^{\mathcal{N}}(\boldsymbol{\mu})$ for all $\boldsymbol{\mu}$ can be done efficiently using the so-called Successive Constraint Method and related approaches^{26,27,28,29,30}. As to the dual norm of the residual $r_N(\cdot; \boldsymbol{\mu}) \in (X^{\mathcal{N}})'$, we also take advantage of a suitable offline-online splitting. In fact, we first invoke the Riesz representation theorem and define functions $\mathcal{C}^q, \mathcal{L}_i^q \in X^{\mathcal{N}}$ such that

$$\begin{cases} (\mathcal{C}^q, v)_{X^{\mathcal{N}}} = f^q(v)_{X^{\mathcal{N}}} \quad \forall v \in X^{\mathcal{N}}, 1 \leq q \leq Q_f \\ (\mathcal{L}_i^q, v)_{X^{\mathcal{N}}} = a^q(u^{\mathcal{N}}(\boldsymbol{\mu}^i), v) \quad \forall v \in X^{\mathcal{N}}, 1 \leq q \leq Q_a, 1 \leq i \leq N. \end{cases} \quad (14)$$

¹In actual computation, we orthonormalize the basis $\{u^{\mathcal{N}}(\boldsymbol{\mu}^i)\}$ through a Gram-Schmidt procedure for numerical stability.

Notice that problem (14) is parameter-independent, hence C^q and \mathcal{L}_m^q can be computed offline. Combining (12), (9) and (8), we have

$$\begin{aligned} \|r_N(\cdot; \boldsymbol{\mu})\|_{(X^{\mathcal{N}'})}^2 &= \sum_{q_1=1}^{Q_f} \sum_{\tilde{q}_1=1}^{Q_f} \Theta_f^{q_1}(\boldsymbol{\mu}) \Theta_f^{\tilde{q}_1}(\boldsymbol{\mu}) (C^{q_1}, C^{\tilde{q}_1})_{X^{\mathcal{N}'}} + \\ &\quad \left\{ \sum_{q_2=1}^{Q_a} \sum_{i=1}^N \Theta_a^{q_2}(\boldsymbol{\mu}) u_{Ni}^{\mathcal{N}} \left\{ \sum_{q'_2=1}^{Q_a} \sum_{i'=1}^N \Theta_a^{q'_2}(\boldsymbol{\mu}) u_{Ni'}^{\mathcal{N}} (\mathcal{L}_i^{q_2}, \mathcal{L}_{i'}^{q'_2})_{X^{\mathcal{N}'}} \right\} \right\} \\ &\quad - 2 \sum_{q_2=1}^{Q_a} \sum_{i=1}^N \sum_{q_1=1}^{Q_f} \Theta_a^{q_2}(\boldsymbol{\mu}) u_{Ni}^{\mathcal{N}} (\mathcal{L}_i^{q_2}, C^{q_1})_{X^{\mathcal{N}'}} \end{aligned} \quad (15)$$

where the parameter-independent quantities $(C^{q_1}, C^{\tilde{q}_1})_{X^{\mathcal{N}'}}$, $(C^{q_1}, \mathcal{L}_i^{q_2})_{X^{\mathcal{N}'}}$, $(\mathcal{L}_i^{q_2}, \mathcal{L}_{i'}^{q'_2})_{X^{\mathcal{N}'}}$, $1 \leq i, i' \leq N_{\text{RB}}$, $1 \leq q_1, \tilde{q}_1 \leq Q_f$, $1 \leq q_2, q'_2 \leq Q_a$ can be precomputed and stored. Once we can efficiently calculate $\Delta_n(\boldsymbol{\mu})$, the classical greedy algorithm, outlined in Algorithm 1 is invoked to build the parameter set S_N and the resulting reduced basis space $X_N^{\mathcal{N}'}$.

Algorithm 1 Classical Greedy, $(N, X_N^{\mathcal{N}'}) = \mathbb{C}\mathbb{G}(\Xi_{\text{train}}, \epsilon_{\text{tol}}, N, X_N^{\mathcal{N}'})$

- 1: **if** $N = 0$ **then**
 - 2: Initialization: Choose an initial parameter value $\boldsymbol{\mu}^1 \in \Xi_{\text{train}}$, set $S_1 = \{\boldsymbol{\mu}^1\}$, compute $u^{\mathcal{N}}(\boldsymbol{\mu}^1)$, and let $X_N^{\mathcal{N}'} = \{u^{\mathcal{N}}(\boldsymbol{\mu}^1)\}$
 $N = 1$;
 - 3: **end if**
 - 4: **while** $\max_{\boldsymbol{\mu} \in \Xi_{\text{train}}} \Delta_N(\boldsymbol{\mu}) > \epsilon_{\text{tol}}$ **do**
 - 5: Choose $\boldsymbol{\mu}^{N+1} = \operatorname{argmax}_{\boldsymbol{\mu} \in \Xi_{\text{train}}} \Delta_N(\boldsymbol{\mu})$;
 - 6: $S_{N+1} = S_N \cup \{\boldsymbol{\mu}^{N+1}\}$;
 - 7: Compute $u^{\mathcal{N}}(\boldsymbol{\mu}^{N+1})$ and augment RB space $X_{N+1}^{\mathcal{N}'} = X_N^{\mathcal{N}'} \oplus \{u^{\mathcal{N}}(\boldsymbol{\mu}^{N+1})\}$.
 - 8: $N \leftarrow N + 1$.
 - 9: **end while**
-

2.2 | Existing offline enhancement strategies

The greedy algorithm $\mathbb{C}\mathbb{G}(\Xi_{\text{train}}, \epsilon_{\text{tol}}, N, X_N^{\mathcal{N}'})$ requires maximization of the *a posteriori* error estimate over Ξ_{train} . This becomes a bottleneck in the construction of the RB space $X_N^{\mathcal{N}'}$, especially when the parameter domain \mathcal{D} is of high dimension. Much recent research has developed the schemes capable of accelerating this standard greedy algorithm. In this section, we review three such offline enhancement strategies as proposed in^{12,13,14} in Subsection 2.2.1 to 2.2.3 respectively. The improved greedy algorithms are described in Algorithms 2 to 4 accordingly.

2.2.1 | A priori training set decomposition (TSD)

In¹², a modified greedy algorithm is provided to address the many-parameter heat conduction problems. It attempts to mitigate the effect of large Ξ_{train} by running the classical greedy algorithm first on a relatively small training set before attempting to sequentially augment the reduced basis space in larger training sets. To do so, they decompose the full training set Ξ_{train} into a sequence of mutually exclusive subsets $\{\Xi_{\text{train},1}, \dots, \Xi_{\text{train},\mathcal{J}}\}$ that has $\{\Xi_{\text{train},1}, \dots, \Xi_{\text{train},\mathcal{J}-1}\}$ increasing in size geometrically and the last one ensuring that the whole training set is covered, i.e. $\Xi_{\text{train},1} \cup \dots \cup \Xi_{\text{train},\mathcal{J}} = \Xi_{\text{train}}$. The main idea is running the greedy algorithm over the small sets would result in a basis capable of resolving a large portion of the larger sets. These portions, i.e. the samples whose current error estimator is below the tolerance, will be skipped thereby increasing the speed of the greedy scan. The TSD algorithm includes a final run on Ξ_{train} as a sanity check.

The size of the first sample set $n_{\text{tr,small}} = |\Xi_{\text{train},1}|$ serves as the (only) tuning parameter for this approach. As an example to build up this partition, let $\mathcal{J} = \text{floor}(\log_2(\frac{n_{\text{train}}}{n_{\text{tr,small}}}))$. For $j = 2 : \mathcal{J} - 1$, $|\Xi_{\text{train},j}| = 2^{j-1}n_{\text{tr,small}}$. The size of $\Xi_{\text{train},\mathcal{J}}$ equals to $n_{\text{train}} - \sum_{j=1}^{\mathcal{J}-1} |\Xi_{\text{train},j}|$. To make each of the subsets span the whole training set, the algorithm randomly sample $n_{\text{train},j}$ points from Ξ_{train} . For j -th sample set, the *a posteriori* error estimate computed by N reduced bases is denoted as $\Delta_{N,j}(\boldsymbol{\mu})$. The pseudo-code of this methodology is provided in algorithm 2.

Remark 1. This approach has $n_{\text{tr,small}}$ as the only tuning parameter. Small $n_{\text{tr,small}}$ likely leads to higher dimension of the surrogate solution space negatively impacting the online efficiency. Therefore, we usually choose relatively large $n_{\text{tr,small}}$ in comparison to n_{train} . Unfortunately, large $n_{\text{tr,small}}$ will lead to more costly offline stage. This is obvious since when, in the extreme case, $n_{\text{tr,small}} = n_{\text{train}}$, Algorithm 2 is exactly the same as classical greedy algorithm. This balance of tuning the parameter $n_{\text{tr,small}}$ is rather intricate, as shown by our second numerical experiment in Section 4.1. In comparison, our proposed adaptive approaches are much less sensitive to their tuning parameters.

Algorithm 2 Training set decomposition based classical greedy $(N, X_N^{\mathcal{N}}) = \text{TSD_CG}(\Xi_{\text{train}}, \epsilon_{\text{tol}})$

- 1: Determine a partition $\{\Xi_{\text{train},j}\}_{j=1}^{\mathcal{J}}$ for Ξ_{train} , e.g. by randomly sampling $n_{\text{train},j}$ points from Ξ_{train} to form $\Xi_{\text{train},j}$ where $|\Xi_{\text{train},j}| = 2^{j-1}n_{\text{tr,small}}$ for $j = 1, \dots, \mathcal{J} - 1$, and $\Xi_{\text{train},\mathcal{J}}$ completing the partition.
 - 2: Let $N = 0$.
 - 3: **for** $j = 1 : \mathcal{J}$ **do**
 - 4: Call $(N, X_N^{\mathcal{N}}) = \text{CG}(\Xi_{\text{train},j}, \epsilon_{\text{tol}}, N, X_N^{\mathcal{N}})$
 - 5: **end for**
-

2.2.2 | Adaptive enriching

To avoid running standard greedy algorithm multiple times on the large training set, the adaptive enriching algorithm¹³ opts for executing the greedy algorithm on a dynamically determined subset of the full training set that is fixed in size much smaller than the full training set. The sample set is iteratively updated, after each greedy step, by removing parameters that have error estimate below the tolerance and randomly adding new parameter values from the training set. The rationale is that it is not worthwhile to keep those parameters whose corresponding surrogate solutions are already accurate enough. The size of the sample set is always maintained at a fixed number M_{sample} that needs to be specified by practitioners. More details of this algorithm are provided in Algorithm 3. Since the maximum *a posteriori* error estimate in the stopping criteria is only the maximum in sample set rather than full training set, a safety check step is introduced to ensure each parameter of the full training set is checked once. For problems that we don't have monotonic decay of error or error estimate for, a final "check" over the entire training set is necessary.

Remark 2. The adaptive enriching scheme has one tuning parameter M_{sample} . Two extremal cases are worth mentioning:

- When $M_{\text{sample}} = 1$, the method becomes the approach taken by³¹ and³² where each parameter is examined once and decision on keep or toss made immediately. This approach may result in a larger-than-necessary surrogate space.
- When $M_{\text{sample}} = n_{\text{train}}$, this algorithm is identical to the classical greedy algorithm, thus no savings are realized.

Furthermore, a tuning parameter test of this algorithm for the many-parameter heat conduction problem is presented in Section 4.1, which indicates that the performance of this approach is again rather sensitive to the choice of its tuning parameter M_{sample} .

2.2.3 | Adaptive construction of surrogate training sets

The offline-enhanced RBMs of¹⁴ adaptively identifies a subset of the training set, termed a "Surrogate Training Set" (STS), on which to perform the classical greedy algorithm. Its distinctive feature is that the construction of STS is informed by the error estimator $\{\Delta_n(\boldsymbol{\mu}) : \boldsymbol{\mu} \in \Xi_{\text{train}}\}$ while the methods in^{12,13} are not. After every sweep of the full parameter domain Ξ_{train} via

Algorithm 3 Adaptive enriching classical greedy $(N, X_N^{\mathcal{N}}) = \text{AE_CG}(\Xi_{\text{train}}, \epsilon_{\text{tol}}, M_{\text{sample}})$

- 1: $N_{\text{safe}} = \text{ceil}(|\Xi_{\text{train}}|/M_{\text{sample}})$;
 - 2: Randomly generate an initial training set Ξ with M_{sample} parameters from Ξ_{train} ;
 - 3: Choose an initial parameter $\mu^1 \in \Xi$. Set $S_1 = \{\mu^1\}$, $X_1^{\mathcal{N}} = \text{span}\{u^{\mathcal{N}}(\mu^1)\}$ and $N = 1$;
 - 4: Set $\text{safe} = 0$, $\epsilon = 2\epsilon_{\text{tol}}$ and $r = n_{\text{train}}$;
 - 5: **while** ($\epsilon > \epsilon_{\text{tol}}$ or $\text{safe} \leq N_{\text{safe}}$) and ($r > 0$) **do**
 - 6: Choose $\mu^{N+1} = \underset{\mu \in \Xi}{\text{argmax}} \Delta_N(\mu)$;
 - 7: Augment RB space $X_{N+1}^{\mathcal{N}} = X_N^{\mathcal{N}} \oplus \{u^{\mathcal{N}}(\mu^{N+1})\}$, $S_{N+1} = S_N \cup \{\mu^{N+1}\}$;
 - 8: Truncate Ξ by $\Xi_{<\epsilon} = \{\mu \in \Xi : \Delta_N(\mu) < \epsilon_{\text{tol}}\}$.
 - 9: Truncate Ξ_{train} by $\Xi_{<\epsilon}$, and set $r = r - |\Xi_{<\epsilon}|$;
 - 10: **if** $|\Xi_{<\epsilon}| = M_{\text{sample}}$ **then**
 - 11: Set $\text{safe} = \text{safe} + 1$.
 - 12: **end if**
 - 13: Randomly choose $M_{\text{sample}} - |\Xi|$ parameters from Ξ_{train} for addition to Ξ ;
 - 14: Set $N \leftarrow N + 1$;
 - 15: **end while**
-

performing $\mu^{N+1} = \underset{\mu \in \Xi_{\text{train}}}{\text{argmax}} \Delta_N(\mu)$, a much smaller STS Ξ_{sur} is constructed and then the classical greedy is invoked on the STS until it is deemed as fully resolved, i.e. $\max_{\mu \in \Xi_{\text{sur}}} \Delta_N(\mu)$ is below the tolerance. At that point, Ξ_{train} is examined again by performing the maximization over Ξ_{train} to start the next cycle. These surrogate sets are significantly smaller than the full training set, yet selected well enough to capture the general landscape of the error-estimate manifold. Thus, one attraction of this approach is its unique algorithmic structure, shown in Algorithm 4, of error estimate-informed transition between the full and surrogate training sets. The frequent targeted searches over STS produce a potential relative saving of $1 - |\Xi_{\text{sur}}|/|\Xi_{\text{train}}|$. The reason is that these searches are operated on STS Ξ_{sur} instead of on Ξ_{train} , and that the cost of these searches is linearly dependent on the size of the set it operates on.

We adopt the more cost effective of the two strategies from ¹⁴ for building STS, the Successive Maximization Method (SMM). SMM is inspired by inverse transform sampling for non-standard univariate probability distributions. Indeed, motivated by the notion that the difference between the norm of the errors $\|e(\mu_1)\|_X - \|e(\mu_2)\|_X$ is partially indicative of the difference between the solutions. When selecting the $(N + 1)$ -th parameter value, we construct STS by equidistantly sampling values from $\Delta_N(\Xi_{\text{train}})$. With ϵ_{tol} the stopping tolerance for the RB sweep, let $\Delta_N^{\text{max}} = \max_{\mu \in \Xi_{\text{train}}} \Delta_N(\mu)$. We define $I_N^{M_\ell}$ as an equi-spaced set between ϵ_{tol} and Δ_N^{max} :

$$I_N^{M_\ell} = \left\{ v_{N,m} := \epsilon_{\text{tol}} + (\Delta_N^{\text{max}} - \epsilon_{\text{tol}}) \frac{m}{M_\ell} : m = 0, \dots, M_\ell - 1 \right\}. \quad (16)$$

Roughly speaking, we attempt to construct Ξ_{sur} as $\Xi_{\text{sur}} = \Delta_N^{-1}(I_N^{M_\ell}) \cap \Xi_{\text{train}}$. On outer loop round ℓ , we have $|\Xi_{\text{sur}}| \leq M_\ell$ by this construction, where M_ℓ can be chosen as any monotonically increasing function with respect to ℓ . But in order to avoid excessively large Ξ_{sur} , we set $M_\ell = C_M(\ell + 1)$, where C_M is a constant. After this construction, we repeatedly sweep the current Ξ_{sur} until

$$\max_{\mu \in \Xi_{\text{sur}}} \Delta_N(\mu) \leq E_\ell \frac{1}{((\ell + 1) \times K_{\text{damp}})},$$

where E_ℓ is the starting (global) maximum error estimate for this outer loop iteration. The damping ratio for outer loop ℓ , $\frac{1}{(\ell + 1) \times K_{\text{damp}}}$, enforces that the maximum error estimate over the Ξ_{sur} decreases by a damping factor controlled by K_{damp} which should be determined by the practitioner and the problem at hand. Following the choice in ¹⁴, we take K_{damp} to be constant in this paper. Algorithm 4 details the adaptively constructed STS approach.

Remark 3. This approach has two tuning parameters C_M and K_{damp} . The choice of C_M indirectly controls the size of Ξ_{sur} . These surrogate training sets should be small enough compared to the full one Ξ_{train} to offer considerable acceleration of the greedy sweep, yet large enough to capture the general landscape of the solution manifold that is iteratively learned. On the other hand, K_{damp} controls how accurate we intend to resolve $u_N^{\mathcal{N}}(\mu)$, where $\mu \in \Xi_{\text{sur}}$. The larger C_M and K_{damp} are, the faster algorithm 4

will be. As will be shown by the tuning parameter study in Section 4.1, the efficiency of this approach is less sensitive to the choice of its tuning parameters.

Algorithm 4 Adaptively constructed STS based classical greedy $(N, X_N^{\mathcal{N}}) = \text{STS_CG}(\Xi_{\text{train}}, \epsilon_{\text{tol}}, C_M, K_{\text{damp}}, N, X_N^{\mathcal{N}})$

```

1: if  $N = 0$  then
2:   Randomly select the first sample  $\mu^1 \in \Xi_{\text{train}}$ , and set  $N = 1$ ,  $\ell = 0$  and  $E_0 = 2\epsilon_{\text{tol}}$ ;
3:   Obtain truth solution  $u^{\mathcal{N}}(\mu^1)$ , and set  $S_1 = \{\mu^1\}$ ,  $X_1^{\mathcal{N}} = \text{span}\{u^{\mathcal{N}}(\mu^1)\}$ ;
4: end if
5: while  $(E_\ell > \epsilon_{\text{tol}})$  do
6:   Set  $\ell \leftarrow \ell + 1$ ;
7:   One-step greedy
   scan on  $\Xi_{\text{train}}$ 
   8:   for each  $\mu \in \Xi_{\text{train}}$  do
   9:     Obtain RBM solution  $u_N^{\mathcal{N}}(\mu) \in X_N^{\mathcal{N}}$  and error estimate  $\Delta_N(\mu)$ ;
   10:   end for
   11:    $\mu^{N+1} = \underset{\mu \in \Xi_{\text{train}}}{\text{argmax}} \Delta_N(\mu)$ ,  $\epsilon = \Delta_N(\mu^{N+1})$ ,  $E_\ell = \epsilon$ ;
   12:   Augment RB space  $X_{N+1}^{\mathcal{N}} = X_N^{\mathcal{N}} \oplus \{u^{\mathcal{N}}(\mu^{N+1})\}$ ;
   13:    $S_{N+1} = S_N \cup \{\mu^{N+1}\}$ ;
   14:   Set  $N \leftarrow N + 1$ ;
15:   Construct STS  $\Xi_{\text{Sur}}$  based on  $\{(u_{N-1}^{\mathcal{N}}(\mu), \Delta_{N-1}(\mu)) : \mu \in \Xi_{\text{train}}\}$  with SMM;
   Multi-step greedy
   scan on  $\Xi_{\text{Sur}}$ 
   17:   while  $(\epsilon > \epsilon_{\text{tol}})$  and  $(\frac{\epsilon}{E_\ell} > \frac{1}{K_{\text{damp}} \times (\ell + 1)})$  do
   18:     for each  $\mu \in \Xi_{\text{Sur}}$  do
   19:       Obtain RBM solution  $u_N^{\mathcal{N}}(\mu) \in X_N^{\mathcal{N}}$  and error estimate  $\Delta_N(\mu)$ ;
   20:     end for
   21:      $\mu^{N+1} = \underset{\mu \in \Xi_{\text{Sur}}}{\text{argmax}} \Delta_N(\mu)$ ,  $\epsilon = \Delta_N(\mu^{N+1})$ ;
   22:     Augment RB space  $X_{N+1}^{\mathcal{N}} = X_N^{\mathcal{N}} \oplus \{u^{\mathcal{N}}(\mu^{N+1})\}$ ;
   23:      $S_{N+1} = S_N \cup \{\mu^{N+1}\}$ ;
   24:     Set  $N \leftarrow N + 1$ ;
   25:   end while
26: end while

```

3 | HYBRID OFFLINE ENHANCEMENTS FOR THE GREEDY ALGORITHMS

The unifying theme of the three approaches in the previous section is the construction of a small-size subset of the full training set on which the classical greedy algorithm is performed. Algorithm 4 takes full advantage of these information when constructing the small subsets. Nonetheless, the construction of the surrogate training sets relying on the evaluation of $\Delta_N(\mu)$ for all μ in the training set Ξ_{train} is still a bottleneck of Algorithm 4. Algorithms 2 and 3 do not rely on $\Delta_N(\mu)$ and construct the subset by randomly choosing parameters in Ξ_{train} . However, determining the size of the subset becomes tricky. Too small a subset will degrade the online efficiency, but a very large subset will hinder the offline speed. Motivated by the thought of combining the strengths of both types of algorithms, we develop the following two hybrid algorithms. Indeed, we start with Algorithm 2 or 3 while choosing a relatively large initial subset. We then adopt the idea of Algorithm 4 to build up surrogate training set Ξ_{sur} by computing the *a posteriori* error estimate of the parameters in this subset. Next, we details these two hybrid algorithms.

Hybrid Training Set Decomposition

The idea of Algorithm 2 is to decompose the full training set Ξ_{train} into small subsets $\{\Xi_{\text{train},j}\}_{j=1}^J$ and then run standard greedy algorithm on each of them sequentially from $\Xi_{\text{train},1}$ to $\Xi_{\text{train},J}$. Since, in practical examples, most snapshots are chosen when

performing the classical greedy algorithm on $\Xi_{\text{train},1}$, $\Xi_{\text{train},1}$ can not be too small relative to the full training set. Otherwise, it is not rich enough to emulate the full training set. However, large $\Xi_{\text{train},1}$ increases the offline cost significantly. Our first hybrid method, Algorithm 5 integrating Algorithms 2 and 4, mitigates this dilemma by running Algorithm 4 in each of the subsets generated by the training set decomposition $\{\Xi_{\text{train},j}\}_{j=1}^{\mathcal{J}}$.

That is, given a full training set Ξ_{train} , first we construct a training set decomposition according to Algorithm 2 to obtain $\{\Xi_{\text{train},j}\}_{j=1}^{\mathcal{J}}$. Then, we perform algorithm 4 on each sample set $\Xi_{\text{train},j}$ sequentially. As verified by our numerical results, this simple hybrid approach tends to reduce the greedy algorithm's sensitivity to $n_{\text{tr,small}}$, while retaining the ease of picking C_M and K_{damp} as outlined in section 2.2.3.

Algorithm 5 Hybrid training set decomposition-based greedy algorithm $(N, X_N^{\mathcal{N}}) = \text{H_TSD_CG}(\Xi_{\text{train}}, \epsilon_{\text{tol}}, C_M, K_{\text{damp}})$

- 1: Determine a partition $\{\Xi_{\text{train},j}\}_{j=1}^{\mathcal{J}}$ for Ξ_{train} , e.g. by randomly sampling $n_{\text{train},j}$ points from Ξ_{train} to form $\Xi_{\text{train},j}$ where $|\Xi_{\text{train},j}| = 2^{j-1}n_{\text{tr,small}}$ for $j = 1, \dots, \mathcal{J} - 1$, and $\Xi_{\text{train},\mathcal{J}}$ completing the partition.
 - 2: Choose $\mu^1 \in \Xi_{\text{train},1}$ at random. Denote $S_1 = \{\mu^1\}$, $X_1^{\mathcal{N}} = \text{span}\{u^{\mathcal{N}}(\mu^1)\}$ and $N = 1$;
 - 3: **for** $j = 1 : \mathcal{J}$ **do**
 - 4: Call $(N, X_N^{\mathcal{N}}) = \text{STS_CG}(\Xi_{\text{train},j}, \epsilon_{\text{tol}}, C_M, K_{\text{damp}}, N, X_N^{\mathcal{N}})$
 - 5: **end for**
-

Hybrid Adaptive Enriching

The randomly-generated sample set Ξ in Algorithm 3, albeit not covering all of Ξ_{train} , keeps updating itself after each round of greedy searching by replacing parameter values whose *a posteriori* error estimate falls below ϵ_{tol} by those not seen yet. To avoid having too many rounds of replacements, Ξ must be rich enough to be representative of Ξ_{train} . However, large Ξ adversely impact the algorithm's efficiency. The proposed hybrid strikes a balance between efficiency and richness. Toward that end and as outlined in Algorithm 6, assimilating Algorithms 3 and 4, we adaptively construct Ξ_{sur} for the active training set Ξ which is only fully examined when (the much smaller) Ξ_{sur} is sufficiently resolved. This three-level approach enables a faster examination of Ξ than the Adaptive Enriching algorithm 3 which, in turn, allows Ξ to be larger thus more representative of Ξ_{train} .

Remark 4. As pointed out in Sections 2.2.1 and 2.2.2 and shown in the numerical results section, the performance of the non-hybrid Algorithms 2 and 3 exhibit high sensitivity with respect to the tuning parameters. A direct consequence is that selecting an appropriate tuning parameter is not easy. As will be shown in the numerical results section, their hybrid version Algorithms 5 and 6 not only come with computational acceleration but also are capable of significantly reducing the sensitivity of the tuning parameters thus making the methods more usable.

4 | NUMERICAL TESTS

In this section, we test and compare these six greedy algorithms, namely classical greedy, three existing improvements reviewed in section 2, and our newly designed two hybrids in section 3. For the sake of clarity, we list these methods in one place, Table 2.

Two types of examples will be presented to demonstrate the efficiency enhancement of our proposed approaches without sacrificing the quality of the reduced bases. The corresponding results are presented in the subsections below. The CPU times reported in this paper refer to computations performed on a workstation with 3.1 GHz Intel Core i5 processor and 16GB memory, in the MATLAB environment adopting redbKIT library^{33,1} and RBmatlab package^{34,35,2}.

²Available for download at <http://www.ians.uni-stuttgart.de/MoRePaS/software/index.html>

Algorithm 6 Hybrid adaptive enriching greedy algorithm $\mathbb{H_AE_CG}(\Xi_{\text{train}}, \varepsilon_{\text{tol}}, C_M, K_{\text{damp}}, M_{\text{sample}})$

```

1:  $N_{\text{safe}} = \text{ceil}(|\Xi_{\text{train}}|/M_{\text{sample}})$ ;
2: Randomly generate an initial training set  $\Xi$  with  $M_{\text{sample}}$  parameters from  $\Xi_{\text{train}}$ ;
3: Choose an initial parameter  $\mu^1 \in \Xi_{\text{train}}$ . Set  $S_1 = \{\mu^1\}$ ,  $X_1^{\mathcal{N}} = \text{span}\{u^{\mathcal{N}}(\mu^1)\}$  and  $N = 1$ ;
4: Set  $\text{safe} = 0$ ,  $\ell = 1$ ,  $\varepsilon = 2\varepsilon_{\text{tol}}$  and  $r = n_{\text{train}}$ ;
5: while ( $E_\ell > \varepsilon_{\text{tol}}$  or  $\text{safe} \leq N_{\text{safe}}$ ) and ( $r > 0$ ) do
    7:   for each  $\mu \in \Xi$  do
    8:     Obtain RBM solution  $u_N^{\mathcal{N}}(\mu) \in X_N^{\mathcal{N}}$  and error estimate  $\Delta_N(\mu)$ ;
    9:   end for
10:   $\mu^{N+1} = \underset{\mu \in \Xi}{\text{argmax}} \Delta_N(\mu)$ ,  $\varepsilon = \Delta_N(\mu^{N+1})$ ,  $E_\ell = \varepsilon$ ;
11:  Augment RB space  $X_{N+1}^{\mathcal{N}} = X_N^{\mathcal{N}} \oplus \{u^{\mathcal{N}}(\mu^{N+1})\}$ ;
12:   $S_{N+1} = S_N \cup \{\mu^{N+1}\}$ ;
13:  Set  $N \leftarrow N + 1$ ;
14:  Construct STS  $\Xi_{\text{Sur}}$  based on  $\{(u_{N-1}^{\mathcal{N}}(\mu), \Delta_{N-1}(\mu)) : \mu \in \Xi\}$  with SMM;
16:  while ( $\varepsilon > \varepsilon_{\text{tol}}$ ) and ( $\frac{\varepsilon}{E_\ell} > \frac{1}{K_{\text{damp}} \times (\ell+1)}$ ) do
17:    for each  $\mu \in \Xi_{\text{Sur}}$  do
18:      Obtain RBM solution  $u_N^{\mathcal{N}}(\mu) \in X_N^{\mathcal{N}}$  and error estimate  $\Delta_N(\mu)$ ;
19:    end for
20:     $\mu^{N+1} = \underset{\mu \in \Xi_{\text{Sur}}}{\text{argmax}} \Delta_N(\mu)$ ,  $\varepsilon = \Delta_N(\mu^{N+1})$ ;
21:    Augment RB space  $X_{N+1}^{\mathcal{N}} = X_N^{\mathcal{N}} \oplus \{u^{\mathcal{N}}(\mu^{N+1})\}$ ;
22:     $S_{N+1} = S_N \cup \{\mu^{N+1}\}$ ;
23:    Set  $N \leftarrow N + 1$ ;
24:  end while
25:  Truncate  $\Xi$  by  $\Xi_{<\varepsilon} = \{\mu \in \Xi : \Delta_N(\mu) < \varepsilon_{\text{tol}}\}$ ;
26:  Truncate  $\Xi_{\text{train}}$  by  $\Xi_{<\varepsilon}$ , and set  $r = r - |\Xi_{<\varepsilon}|$ ;
27:  if  $|\Xi_{<\varepsilon}| = M_{\text{sample}}$  then
28:    Set  $\text{safe} = \text{safe} + 1$ , and  $\ell = 1$ ;
29:  else
30:     $\ell = \ell + 1$ ;
31:  end if
32:  Randomly choose  $M_{\text{sample}} - |\Xi|$  parameters from  $\Xi_{\text{train}}$  for addition to  $\Xi$ ;
33: end while

```

4.1 | Thermal Block problem with nine parameters

We start with the classical thermal block problem^{3,1,12,14}.

$$\begin{cases} -\nabla \cdot (a(x, \mu) \nabla u(x, \mu)) = f & \text{on } \Omega, \\ u(x, \mu) = g_D & \text{on } \Gamma_D, \\ \frac{\partial u}{\partial n} = g_N & \text{on } \Gamma_N. \end{cases} \quad (17)$$

Here, $\Omega = [0, 1] \times [0, 1]$ is partitioned into 9 blocks $\bigcup_{i=1}^9 B_i = \Omega$, Γ_D is the top boundary, and $\Gamma_N = \partial\Omega \setminus \Gamma_D$. The heat conductivities on these blocks constitute the parameters of our test:

Γ_D		
$\mu_7(B_7)$	$\mu_8(B_8)$	$\mu_9(B_9)$
$\mu_4(B_4)$	$\mu_5(B_5)$	$\mu_6(B_6)$
$\mu_1(B_1)$	$\mu_2(B_2)$	$\mu_3(B_3)$
Γ_{base}		

Abbrv	Full name
CG	Classical greedy algorithm
TSD_CG	Classical greedy enhanced by Training Set Decomposition
AE_CG	Classical greedy enhanced by Adaptive Enriching
STS_CG	Classical greedy enhanced by adaptively constructed Surrogate Training Set
H_TSD_CG	Hybrid training set decomposition based greedy algorithm
H_AE_CG	Hybrid adaptive enriching greedy algorithm

TABLE 2 Abbreviation of the greedy algorithms used in this section.

That is, the diffusion coefficient $a(x, \boldsymbol{\mu}) = \mu_i$ when $x \in B_i$. The parameter vector is thus given by $\boldsymbol{\mu} = (\mu_1, \mu_2, \dots, \mu_9)$ whose domain is chosen as $\mathcal{D} = [0.1, 10]^9$ for our test. We take as the right hand side $f = 0$. The Dirichlet boundary is set to be homogeneous, i.e. $g_D = 0$. The Neumann data is set to simulate heat influx only at the bottom, i.e. $g_N = 1$ on the bottom boundary Γ_{base} and $g_N = 0$ at the two sides. The output of interest is defined to be the average temperature over Γ_{base}

$$s(\boldsymbol{\mu}) = \int_{\Gamma_{\text{base}}} u(x, \boldsymbol{\mu}) dx. \quad (18)$$

The truth approximation is obtained by a finite element solver^{34,35} with total degrees of freedom $\mathcal{N} = 361$. A sufficient number of samples ($N_{\text{train}} = 4 \times 10^6$) are randomly drawn from the parameter domain \mathcal{D} . The testing set contains another 1,000 random samples in \mathcal{D} . The error is measured in H^1 norm the largest of which is recorded to show the worst case scenario. Moreover, to gain an understanding of the probabilistic nature of the algorithms, we run each of the TSD_CG, AE_CG, H_TSD_CG, H_AE_CG 5 times for every fixed tuning parameter and tabulate the corresponding ranges.

First, we fix $K_{\text{damp}} = 20$, $C_M = 20$, $N_{\text{sample}} = 2 \times 10^5$ and $n_{\text{tr,small}} = 2 \times 10^5$ and test 3 different tolerances. Table 3 shows the accuracy and numbers of bases at convergence for each method, and its speedup factor in comparison to the classical greedy algorithm. For relative time, defined as the corresponding running time scaled by the running time of classical greedy algorithm, we observe that the worst case scenario of the two newly proposed approaches, H_TSD_CG and H_AE_CG, is better than the best case scenario of any other approaches. Moreover, the efficiency is increasing as tolerance gets smaller. Therefore, the alleviation is more pronounced for high-dimensional problem or when high accuracy is desired. In addition, with the same tolerance, the required number of bases are very similar for all these methods. It indicates that offline speedup of both H_TSD_CG and H_AE_CG are not coming at the cost of online efficiency. In terms of accuracy, the worst case (i.e. upper bounds of errors) for H_TSD_CG and H_AE_CG are in the same order of magnitude as the CG. Figure 1 illustrates that the a posteriori error estimate is converging exponentially for both H_TSD_CG and H_AE_CG, in the same fashion as other approaches including the canonical greedy algorithm. This shows that our proposed hybrid algorithms do not appear to suffer accuracy degradation for this example.

Next, we consider the impact of tweaking the tuning parameters. Toward that end, for $\epsilon_{\text{tol}} = 10^{-3}$, we choose $(K_{\text{damp}}, C_M) = (5, 5), (10, 10), (20, 20)$, $N_{\text{sample}} = 1 \times 10^5, 2 \times 10^5, 4 \times 10^5$ and $n_{\text{tr,small}} = 1 \times 10^5, 2 \times 10^5, 4 \times 10^5$ and record the relative time, the numbers of bases at convergence and the RBM error. The results for comparing STS_CG, TSD_CG, AE_CG, H_TSD_CG and H_AE_CG are shown in Table 4, Table 5 and Table 6. For fixed tolerance, it is evident that the performance of the newly proposed H_TSD_CG and H_AE_CG is very stable for various selection of tuning parameters in speed, size of RB space and accuracy. For relative computational time, the largest of the relative time variations (defined as $(t_{\text{max}} - t_{\text{min}})/t_{\text{min}}$) of these two methods is 31%. On the other hand, the efficiency of TSD_CG and AE_CG is severely sensitive of the tuning parameters. In fact, we notice that the setup with the worst tuning parameter settings is half as slow as the that of the optimal setting. Note that although STS_CG is as stable as H_TSD_CG and H_AE_CG, its relative computational time is more than three times higher. Although H_TSD_CG and H_AE_CG are not deterministic, the size of RB space and the accuracy of the resulting reduced solver are both stable with the accuracy being comparable to that of the classical greedy algorithm.

Based on these two experiments, we clearly see that our newly proposed H_TSD_CG and H_AE_CG improve both efficiency and stability. Furthermore, the reduction in tuning parameter sensitivity makes the hybrids particularly attractive.

(a) Efficiency in terms of relative computation time

ϵ_{tol}	CG	STS_CG	TSD_CG	AE_CG	H_TSD_CG	H_AE_CG
10^{-2}	1	0.103	[0.055, 0.057]	[0.061, 0.068]	[0.035, 0.036]	[0.033, 0.034]
10^{-3}	1	0.106	[0.056, 0.063]	[0.060, 0.064]	[0.035, 0.036]	[0.031, 0.032]
10^{-4}	1	0.097	[0.052, 0.053]	[0.058, 0.063]	[0.028, 0.029]	[0.028, 0.029]

(b) Number of bases at convergence

ϵ_{tol}	CG	STS_CG	TSD_CG	AE_CG	H_TSD_CG	H_AE_CG
10^{-2}	50	52	[50, 51]	[50, 51]	[51, 51]	[50, 52]
10^{-3}	60	60	[58, 60]	[59, 60]	[59, 59]	[59, 61]
10^{-4}	65	66	[64, 66]	[65, 65]	[64, 66]	[65, 66]

(c) Accuracy(H^1 norm): (in 10^{-4})

ϵ_{tol}	CG	STS_CG	TSD_CG	AE_CG	H_TSD_CG	H_AE_CG
10^{-2}	1.34	0.84	[1.11, 2.93]	[0.74, 3.11]	[1.04, 1.40]	[1.46, 2.94]
10^{-3}	0.21	0.09	[0.08, 0.44]	[0.11, 0.31]	[0.13, 0.28]	[0.05, 0.22]
10^{-4}	0.009	0.008	[0.008, 0.01]	[0.006, 0.01]	[0.008, 0.01]	[0.006, 0.008]

TABLE 3 Results for the nine-dimensional thermal block problem: (a) Comparison of speedup, (b) size of the resulting reduced basis space, and (c) accuracy.

4.2 | Helmholtz equation on a parametrized domain

For our second test, we turn to a more challenging non-coercive and nonaffine problem which is parameterized by the geometric configuration of the system. Indeed, we consider the propagation of a pressure wave $P(\mathbf{x}, t)$ into the acoustic horn illustrated in Figure 2, the same example considered in³⁶. Assuming that the waves are time harmonic, the acoustic pressure P can be separated as $P(x, t) = \Re(p(x) \exp^{i\omega t})$ where the complex amplitude $p(x)$ satisfies the following Helmholtz equation^{37,36}:

$$\begin{aligned}
 \Delta p + \kappa^2 p &= 0 && \text{in } \Omega \\
 (i\kappa + \frac{1}{2R})p + \nabla p \cdot \mathbf{n} &= 0 && \text{on } \Gamma_o \\
 i\kappa p + \nabla p \cdot \mathbf{n} &= 2i\kappa A && \text{on } \Gamma_i \\
 \nabla p \cdot \mathbf{n} &= 0 && \text{on } \Gamma_h \cup \Gamma_s = \Gamma_n,
 \end{aligned} \tag{19}$$

where $\kappa = \omega/c$ is the wave number, $\omega = 2\pi f$ the angular frequency and $c = 340 \frac{\text{cm}}{\text{s}}$ the speed of sound. A radiation condition is prescribed on the boundary Γ_i imposing an inner-going wave with amplitude $A = 1$ and absorbing the outer-going planar waves. A Neumann boundary condition is applied on the walls Γ_h of the device as well as on the symmetry boundary Γ_s . Finally, an absorbing condition is placed on the far-field boundary Γ_o with radius $R = 1$.

We consider up to five parameters. The first is the frequency f . The other four describe the shape of the horn, representing the vertical displacement of the RBF control points³⁸ in Figure 2. As a result, we have the five-dimensional parameter vector $\mu = [f \quad \mu_g]$. The output of interest is the index of reflection intensity (IRI)³⁹ defined as

$$J(\mu) = \left| \frac{1}{\Gamma_i} \int_{\Gamma_i} p(\mu) d\Gamma - 1 \right|,$$

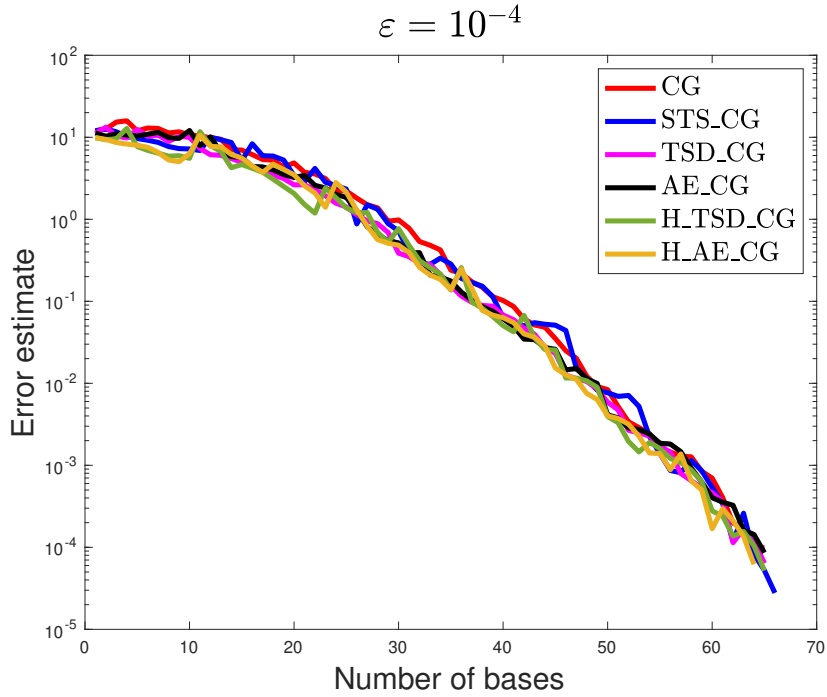


FIGURE 1 Convergence of a posteriori error estimate for the thermal block problem.

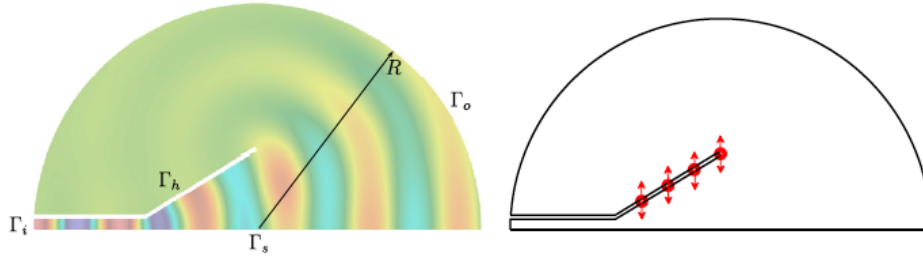


FIGURE 2 Left: the acoustic horn domain and boundaries (background coloring given by $\mathfrak{R}(p)$ for $f = 900\text{Hz}$). Right: RBF control points (red circles) whose vertical displacement is treated as a parameter. [Figure taken from³⁶].

which measures the transmission efficiency of the device. Since the pressure p depends on the design of the horn and the frequency, we parametrized the reference domain Ω and define it as $\Omega(\boldsymbol{\mu}_g)$, where the details of the parametrized construction can be found in^{40,41}. Given $\boldsymbol{\mu} \in \mathcal{D}$, the weak form of problem (19) reads: find $p \in H^1(\Omega(\boldsymbol{\mu}_g))$ such that

$$a(p, v, \boldsymbol{\mu}) = g(v, \boldsymbol{\mu}) \quad \forall v \in H^1(\Omega(\boldsymbol{\mu}_g)), \quad (20)$$

where

$$a(p, v, \boldsymbol{\mu}) = \int_{\Omega(\boldsymbol{\mu}_g)} (\nabla p \cdot \nabla \bar{v} - \kappa^2 p \bar{v}) d\Omega + i\kappa \int_{\Gamma_o \cup \Gamma_i} p \bar{v} d\Gamma + \frac{1}{2R} \int_{\Gamma_o} p \bar{v} d\Gamma, \quad (21)$$

$$g(v, \boldsymbol{\mu}) = 2i\kappa A \int_{\Gamma_i} \bar{v} d\Gamma. \quad (22)$$

We adopt the same implementation as³⁶, i.e. a conforming triangular finite element method discretizing problem (20) by approximating $H^1(\Omega(\boldsymbol{\mu}_g))$ with a set of \mathcal{N} piecewise polynomial nodal basis functions $\{\phi_i\}_{i=1}^{\mathcal{N}}$. Then the FOM solver ends up with solving the following large linear system:

$$\mathcal{A}(\boldsymbol{\mu})\mathbf{p} = \mathbf{g}(\boldsymbol{\mu}), \quad (23)$$

(a) STS_CG			
(K_{damp}, C_M)	(5, 5)	(10, 10)	(20, 20)
	0.129	0.127	0.106
(b) TSD_CG			
$n_{\text{tr,small}}$	1×10^5	2×10^5	4×10^5
	[0.041, 0.047]	[0.056, 0.063]	[0.089, 0.10]
(c) AE_CG			
M_{sample}	1×10^5	2×10^5	4×10^5
	[0.044, 0.045]	[0.060, 0.064]	[0.086, 0.097]
(d) H_TSD_CG			
$(K_{\text{damp}}, C_M)/n_{\text{tr,small}}$	1×10^5	2×10^5	4×10^5
(5, 5)	[0.030, 0.031]	[0.036, 0.037]	[0.037, 0.038]
(10, 10)	[0.030, 0.030]	[0.036, 0.037]	[0.036, 0.037]
(20, 20)	[0.029, 0.030]	[0.035, 0.036]	[0.035, 0.036]
(e) H_AE_CG			
$(K_{\text{damp}}, C_M)/n_{\text{tr,small}}$	1×10^5	2×10^5	4×10^5
(5, 5)	[0.030, 0.031]	[0.032, 0.034]	[0.033, 0.038]
(10, 10)	[0.029, 0.030]	[0.031, 0.032]	[0.035, 0.036]
(20, 20)	[0.029, 0.030]	[0.031, 0.032]	[0.034, 0.035]

TABLE 4 Tuning parameter study for the thermal block problem. Comparison of relative efficiency for various enhanced greedy algorithms.

where

$$A_{ij}(\boldsymbol{\mu}) = a(\phi_j, \phi_i, \boldsymbol{\mu}), \quad (24)$$

$$g_i(\boldsymbol{\mu}) = g(\phi_i, \boldsymbol{\mu}), \quad 1 \leq i, j \leq \mathcal{N}. \quad (25)$$

Many scenarios of this problem, e.g. optimizing the shape for the horn's transmission efficiency, require solving the large system (23) for many different configurations. However, even one such solution can be computationally intensive to obtain due to the nonaffinity of the problem introduced by the geometric parameterization. Indeed, empirical interpolation method^{23,24,25} is usually used to achieve the online independence of the full model degrees of freedom by approximating the non-affine parametrized PDE with a linear combination of Q_a affine terms. Let us consider for instance the matrix corresponding to the first term of (21), $\int_{\Omega(\boldsymbol{\mu}_g)} \nabla p \cdot \nabla \bar{v} d\Omega$.

$$\mathcal{K}_{ij}(\boldsymbol{\mu}_g) = \int_{\Omega(\boldsymbol{\mu}_g)} \nabla \phi_j \cdot \nabla \bar{\phi}_i d\Omega = \int_{\tilde{\Omega}} \mathcal{T}(\mathbf{x}; \boldsymbol{\mu}_g) \nabla \phi_j \cdot \nabla \bar{\phi}_i d\Omega.$$

Here $\tilde{\Omega}$ is (fixed) reference configuration that is mapped to $\Omega(\boldsymbol{\mu}_g)$ through a parametric map

$$\mathbf{F} : \tilde{\Omega} \times \mathcal{D} \rightarrow \mathbb{R}^2 \quad \text{such that} \quad \mathbf{F}(\tilde{\Omega}; \boldsymbol{\mu}_g) = \Omega(\boldsymbol{\mu}_g).$$

The 2×2 matrix $\mathcal{T}(\mathbf{x}; \boldsymbol{\mu}_g)$ can then be evaluated

$$\mathcal{T}(\mathbf{x}; \boldsymbol{\mu}_g) = (\nabla_{\mathbf{x}} \mathbf{F}(\mathbf{x}, \boldsymbol{\mu}_g))^{-1} (\nabla_{\mathbf{x}} \mathbf{F}(\mathbf{x}, \boldsymbol{\mu}_g))^{-T} \left| \nabla_{\mathbf{x}} \mathbf{F}(\mathbf{x}, \boldsymbol{\mu}_g) \right|$$

(a) STS_CG			
(K_{damp}, C_M)	(5, 5)	(10, 10)	(20, 20)
	60	60	60
(b) TSD_CG			
$n_{\text{tr,small}}$	1×10^5	2×10^5	4×10^5
	[59, 60]	[58, 60]	[59, 59]
(c) AE_CG			
M_{sample}	1×10^5	2×10^5	4×10^5
	[59, 60]	[59, 60]	[57, 58]
(d) H_TSD_CG			
$(K_{\text{damp}}, C_M)/n_{\text{tr,small}}$	1×10^5	2×10^5	4×10^5
(5, 5)	[59, 60]	[58, 60]	[59, 61]
(10, 10)	[59, 61]	[59, 62]	[59, 60]
(20, 20)	[59, 60]	[59, 59]	[59, 60]
(e) H_AE_CG			
$(K_{\text{damp}}, C_M)/n_{\text{tr,small}}$	1×10^5	2×10^5	4×10^5
(5, 5)	[59, 62]	[59, 61]	[59, 60]
(10, 10)	[59, 61]	[59, 61]	[59, 60]
(20, 20)	[59, 61]	[59, 61]	[59, 60]

TABLE 5 Tuning parameter study for the thermal block problem. Comparison of number of bases at convergence for various enhanced greedy algorithms.

The EIM approximates each component of $\mathcal{T}(x; \boldsymbol{\mu}_g)$, for any $\boldsymbol{\mu}_g$, by its projection onto a low-dimensional space spanned by some well-chosen instances of $\mathcal{T}(x; \boldsymbol{\mu}_g)$, $\{\mathcal{T}(x; \boldsymbol{\mu}_g) : \boldsymbol{\mu}_g = \boldsymbol{\mu}_g^1, \dots, \boldsymbol{\mu}_g^{Q_{k\ell}}\}$:

$$(\mathcal{T}(x; \boldsymbol{\mu}_g))_{k,\ell} = \sum_{q=1}^{Q_{k\ell}} (\mathcal{T}(x; \boldsymbol{\mu}_g^q))_{k,\ell} \theta(\boldsymbol{\mu}_g).$$

DEIM treats $(\mathcal{T}(x; \boldsymbol{\mu}_g))_{k,\ell}$ with x discretized, thus approximating the $\boldsymbol{\mu}_g$ -dependent $\mathcal{N} \times 1$ vector by a linear combination of $\boldsymbol{\mu}_g$ -independent $\mathcal{N} \times 1$ vectors. This means that, to obtain an affine approximation of $\mathcal{T}(x; \boldsymbol{\mu}_g)$, we need $Q_a = \sum_{k,\ell=1}^2 Q_{k\ell}$ terms. Each $Q_{k\ell}$, and thus the total Q_a , tend to be large when the parameterized operator involves geometrical deformations^{42,43}. As a consequence, the online efficiency, which is dependent on Q_a , is severely degraded. The matrix version of discrete empirical interpolation method (MDEIM)³⁶ partially alleviate the situation by treating the matrix $\mathcal{K}(\boldsymbol{\mu}_g)$ as a whole. That is, it finds Q_a parameter-independent matrices $\mathcal{K}_1, \dots, \mathcal{K}_{Q_a}$

$$\mathcal{K}(\boldsymbol{\mu}_g) = \sum_{q=1}^{Q_a} \mathcal{K}_q \theta_q(\boldsymbol{\mu}_g).$$

This decomposition is achieved by expressing the matrix $\mathcal{K}(\boldsymbol{\mu}_g)$ in vector format via stacking its columns, and then applying DEIM to the resulting ($\boldsymbol{\mu}_g$ -dependent) vector.

However, Q_a is large even with MDEIM³⁶. It is therefore critical to test our newly proposed hybrid methods together with the other offline-enhanced greedy algorithms on this particular problem. Toward that end, we test two different cases. The first case includes two parameters: frequency and one RBF control point, and the second one contains all five parameters $[f \ \boldsymbol{\mu}_g]$.

(a) STS_CG			
(K_{damp}, C_M)	(5, 5)	(10, 10)	(20, 20)
	0.12	0.05	0.09
(b) TSD_CG			
$n_{\text{tr,small}}$	1×10^5	2×10^5	4×10^5
	[0.07, 0.17]	[0.08, 0.4]	[0.11, 0.27]
(c) AE_CG			
M_{sample}	1×10^5	2×10^5	4×10^5
	[0.07, 0.24]	[0.11, 0.31]	[0.25, 0.51]
(d) H_TSD_CG			
$(K_{\text{damp}}, C_M)/n_{\text{tr,small}}$	1×10^5	2×10^5	4×10^5
(5, 5)	[0.08, 0.21]	[0.11, 0.24]	[0.07, 0.37]
(10, 10)	[0.05, 0.18]	[0.04, 0.18]	[0.10, 0.21]
(20, 20)	[0.11, 0.28]	[0.13, 0.28]	[0.19, 0.51]
(e) H_AE_CG			
$(K_{\text{damp}}, C_M)/n_{\text{tr,small}}$	1×10^5	2×10^5	4×10^5
(5, 5)	[0.03, 0.22]	[0.10, 0.24]	[0.11, 0.22]
(10, 10)	[0.09, 0.18]	[0.08, 0.25]	[0.07, 0.28]
(20, 20)	[0.07, 0.19]	[0.05, 0.22]	[0.08, 0.26]

TABLE 6 Tuning parameter study for the thermal block problem. Comparison of algorithmic accuracy for various enhanced greedy algorithms. H^1 norm (in 10^{-4}).

MDEIM³⁶ is applied to obtain the affine approximation, as is done therein. In the numerical experiments, TSD_CG and its corresponding hybrid H_TSD_CG fail for both cases. As a result, we report the comparison of the four algorithms that work, that is CG, STS_CG, AE_CG and H_AE_CG. The detailed setup of both cases are provided in Table 7.

4.2.1 | Two parameters case

We consider frequency and the vertical displacement of the right-most RBF control point in Figure 2. The parameter domain is given by $\mathcal{D} = [50, 1000] \times [-0.03, 0.03]$ and Ξ_{train} is generated by operating Latin hypercube sampling in \mathcal{D} . Other computational parameters are listed in Table 7 second column.

Figure 3 demonstrates the performance of STS_CG, AE_CG and H_AE_CG for five different tolerances $\epsilon_{\text{tol}} = 10^{-3}, 5 \times 10^{-4}, 10^{-4}, 5 \times 10^{-5}, 10^{-5}$. For AE_CG and STS_CG, smaller tolerance leads to more runtime. This is much less severe for H_AE_CG. This observation suggests that H_AE_CG has great potential to handle larger-scale problems. In addition, the sizes of these three RB spaces are very similar, indicating that H_AE_CG does not appear to suffer from online efficiency degradation for this example.

4.2.2 | Five parameters case

We now let all five parameters $[f \ \mu_g]$ vary. The parameter domain is given by $\mathcal{D} = [50, 1000] \times \mathcal{D}_g$, where $\mathcal{D}_g = [-0.03, 0.03]^4$. The full training set Ξ_{train} is also from Latin hypercube sampling in \mathcal{D} . The corresponding computational settings are detailed in Table 7 column 3.

Variable	Value (two parameters)	Value (five parameters)
Size of Ξ_{train}	10000	10000
Number of vertices	4567	4567
Number of elements	8740	8740
Number of nodes	4567	4567
Number of finite element dofs	4567	4567
Interpolation procedure in (8)	MDEIM ³⁶	MDEIM ³⁶
Interpolation points used in (8)	30	250
Number of matrix bases Q_a in (8)	3	95
Number of RHS bases Q_f in (8)	1	4
$(K_{\text{damp}}, C_M, M_{\text{sample}})$	(5, 10, 2048)	(5, 10, 2048)
Tolerance ϵ_{tol}	various	various

TABLE 7 Experiment setup for the acoustic horn.

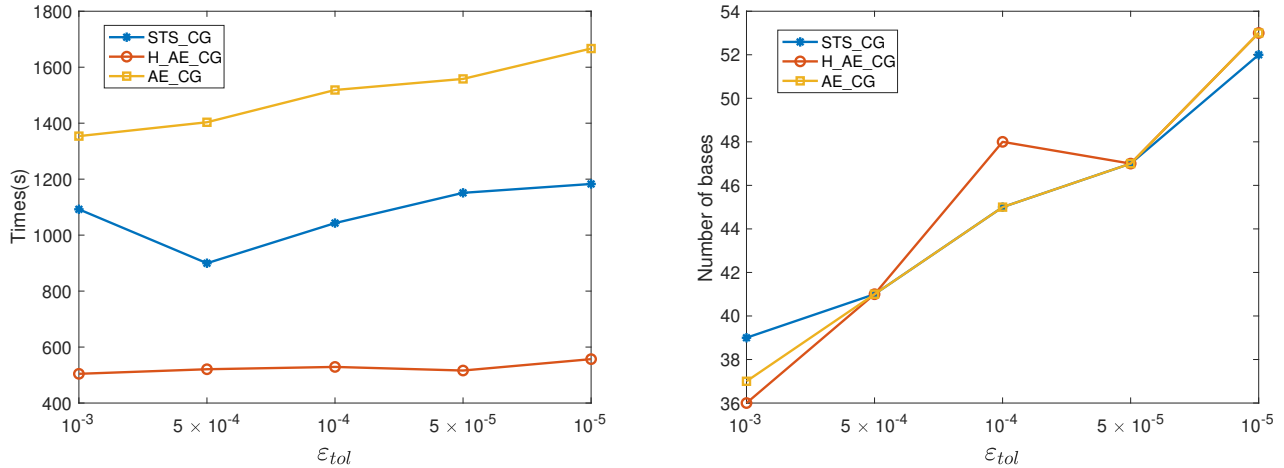


FIGURE 3 Two parameter case for the acoustic horn with different tolerance: computational runtime (left) and number of bases (right).

This five-parameter case is highly non-affine and much more complicated than the previous tests. 95 matrix bases and 4 vector bases are required to approximate this non-affine PDE operator, which significantly increases the computational burden for assembling the reduced solver and evaluating the *a posteriori error estimate*. Due to the computation of CG being much more demanding for this case, we test 3 cases: $\epsilon_{\text{tol}} = 10^{-3}, 5 \times 10^{-4}, 10^{-4}$ to verify the performance of STS_CG, AE_CG and H_AE_CG. The results are shown in Table 8 which demonstrates the efficacy of the new hybrid approach H_AE_CG.

5 | CONCLUSIONS

One of the main computational bottleneck in developing reduced basis methods for parametrized PDEs is the deteriorating offline efficiency for problems with large-scale training set or high-dimensional parameter space. While there are several past attempts to pursue this, these methods still suffer from significant computational cost, and/or lack of robustness resulting from random sampling, and/or sensitivities to the algorithms' tuning parameters.

		(a) Runtime(s)	
Methods/ ϵ_{tol}	10^{-3}	5×10^{-4}	10^{-4}
STS_CG	33849	42903	78998
AE_CG	33779	47473	114030
H_AE_CG	27522	37466	51003

		(a) Number of bases	
Methods/ ϵ_{tol}	10^{-3}	5×10^{-4}	10^{-4}
STS_CG	109	130	193
AE_CG	105	127	187
H_AE_CG	116	135	199

TABLE 8 Results for the five-parameter acoustic horn with different tolerances.

In this paper, we review three recent such offline enhancement approaches for the reduced basis method all of which share the overarching theme of constructing a small-size subset of the full training set and then performing the classical greedy algorithm on it. By closely integrating them, we obtain two new hybrid approaches which are remarkably faster without impacting the quality of reduced basis space. Through two types of different numerical experiments, we demonstrate a significant cost reduction for the offline portion of RBM, robustness, and ease of setting tuning parameters. These experiments lead us to believe that the efficiency will be more pronounced when the non-affinity gets more severe, or the dimension of parameter space gets higher. A detailed follow-up study constitutes our future work.

ACKNOWLEDGMENTS

The authors want to express their sincere gratitude to Prof. Anthony Patera of MIT for suggesting to test the algorithms on the Helmholtz equation. The second author was partially supported by National Science Foundation grant DMS-1719698. This material is based upon work supported by the National Science Foundation under Grant No. DMS-1439786 and by the Simons Foundation Grant No. 50736 while Y. Chen and J. Jiang were in residence at the Institute for Computational and Experimental Research in Mathematics in Providence, RI, during the “Model and dimension reduction in uncertain and dynamic systems” program.

References

1. Quarteroni A, Manzoni A, Negri F. *Reduced basis methods for partial differential equations: An introduction*. 92. Springer . 2015.
2. Hesthaven JS, Rozza G, Stamm B. *Certified reduced basis methods for parametrized partial differential equations*. SpringerBriefs in MathematicsSpringer, Cham; BCAM Basque Center for Applied Mathematics, Bilbao . 2016. BCAM SpringerBriefs
3. Rozza G, Huynh DBP, Patera AT. Reduced basis approximation and a posteriori error estimation for affinely parametrized elliptic coercive partial differential equations. *Arch. Comput. Methods Eng.* 2008; 15(3): 229-275.
4. Haasdonk B. *Chapter 2: Reduced Basis Methods for Parametrized PDEs - A Tutorial Introduction for Stationary and Instationary Problems*: 65-136;
5. Prud'homme C, Rovas D, Veroy K, Maday Y, Patera AT, Turinici G. Reliable real-time solution of parametrized partial differential equations: Reduced-basis output bound methods. *Journal of Fluids Engineering* 2002; 124(1): 70–80.

6. Nguyen NC, Veroy K, Patera AT. Certified Real-Time Solution of Parametrized Partial Differential Equations. In: Yip S., ed. *Handbook of Materials Modeling* Springer Netherlands. 2005 (pp. 1529–1564).
7. Benner P, Gugercin S, Willcox K. A survey of projection-based model reduction methods for parametric dynamical systems. *SIAM review* 2015; 57(4): 483–531.
8. Carlberg K, Bou-Mosleh C, Farhat C. Efficient non-linear model reduction via a least-squares Petrov–Galerkin projection and compressive tensor approximations. *International Journal for Numerical Methods in Engineering* 2011; 86(2): 155–181. doi: 10.1002/nme.3050
9. Carlberg K, Barone M, Antil H. Galerkin v. least-squares Petrov–Galerkin projection in nonlinear model reduction. *Journal of Computational Physics* 2017; 330: 693 - 734. doi: <https://doi.org/10.1016/j.jcp.2016.10.033>
10. Chen Y, Gottlieb S. Reduced Collocation Methods: Reduced Basis Methods in the Collocation Framework.. *J. Sci. Comput.* 2013; 55(3): 718–737.
11. Chen Y, Gottlieb S, Ji L, Maday Y, Xu Z. L1-ROC and R2-ROC: L1- and R2-based Reduced Over-Collocation methods for parametrized nonlinear partial differential equations. *arXiv:1906.07349* 2019.
12. Sen S. Reduced-basis approximation and a posteriori error estimation for many-parameter heat conduction problems. *Numerical Heat Transfer, Part B: Fundamentals* 2008; 54(5): 369–389.
13. Hesthaven JS, Stamm B, Zhang S. Efficient greedy algorithms for high-dimensional parameter spaces with applications to empirical interpolation and reduced basis methods. *ESAIM: Mathematical Modelling and Numerical Analysis* 2014; 48(1): 259–283.
14. Jiang J, Chen Y, Narayan A. Offline-enhanced reduced basis method through adaptive construction of the surrogate training set. *Journal of Scientific Computing* 2017; 73(2-3): 853–875.
15. Haasdonk B, Dihlmann M, Ohlberger M. A training set and multiple bases generation approach for parameterized model reduction based on adaptive grids in parameter space. *Mathematical and Computer Modelling of Dynamical Systems* 2011; 17(4): 423–442.
16. Iapichino L, Quarteroni A, Rozza G. Reduced basis method and domain decomposition for elliptic problems in networks and complex parametrized geometries. *Computers & Mathematics with Applications* 2016; 71(1): 408–430.
17. Urban K, Volkwein S, Zeeb O. Greedy sampling using nonlinear optimization. In: Springer. 2014 (pp. 137–157).
18. Iapichino L, Volkwein S. Optimization strategy for parameter sampling in the reduced basis method. *IFAC-PapersOnLine* 2015; 48(1): 707–712.
19. Ohlberger M, Schindler F. Error control for the localized reduced basis multiscale method with adaptive on-line enrichment. *SIAM Journal on Scientific Computing* 2015; 37(6): A2865–A2895.
20. Kaulmann S, Flemisch B, Haasdonk B, Lie KA, Ohlberger M. The localized reduced basis multiscale method for two-phase flows in porous media. *International Journal for Numerical Methods in Engineering* 2015; 102(5): 1018–1040.
21. Ohlberger M, Rave S, Schindler F. True error control for the localized reduced basis method for parabolic problems. In: Springer. 2017 (pp. 169–182).
22. Zou Z, Kouri D, Aquino W. An adaptive local reduced basis method for solving PDEs with uncertain inputs and evaluating risk. *Computer Methods in Applied Mechanics and Engineering* 2019; 345: 302–322.
23. Barrault M, Nguyen NC, Maday Y, Patera AT. An “empirical interpolation” method: Application to efficient reduced-basis discretization of partial differential equations. *C. R. Acad. Sci. Paris, Série I* 2004; 339: 667–672.
24. Grepl MA, Maday Y, Nguyen NC, Patera AT. Efficient reduced-basis treatment of nonaffine and nonlinear partial differential equations. *Mathematical Modelling and Numerical Analysis* 2007; 41(3): 575–605.

25. Chaturantabut S, Sorensen DC. Nonlinear model reduction via discrete empirical interpolation. *SIAM J. Sci. Comput.* 2010; 32(5): 2737–2764. doi: 10.1137/090766498
26. Huynh DBP, Rozza G, Sen S, Patera AT. A successive constraint linear optimization method for lower bounds of parametric coercivity and inf–sup stability constants. *Comptes Rendus Mathematique* 2007; 345(8): 473–478.
27. Huynh D, Knezevic D, Chen Y, Hesthaven JS, Patera A. A natural-norm successive constraint method for inf-sup lower bounds. *Computer Methods in Applied Mechanics and Engineering* 2010; 199(29-32): 1963–1975.
28. Chen Y. A certified natural-norm successive constraint method for parametric inf–sup lower bounds. *Applied Numerical Mathematics* 2016; 99: 98–108.
29. Yano M. A space-time Petrov–Galerkin certified reduced basis method: Application to the Boussinesq equations. *SIAM Journal on Scientific Computing* 2014; 36(1): A232–A266.
30. Manzoni A, Negri F. Heuristic strategies for the approximation of stability factors in quadratically nonlinear parametrized PDEs. *Advances in Computational Mathematics* 2015; 41(5): 1255–1288.
31. Elman HC, Liao Q. Reduced basis collocation methods for partial differential equations with random coefficients. *SIAM/ASA Journal on Uncertainty Quantification* 2013; 1(1): 192–217.
32. Liu Y, Chen T, Chen Y, Shu CW. Certified Offline-Free Reduced Basis (COFRB) Methods for Stochastic Differential Equations Driven by Arbitrary Types of Noise. *Journal of Scientific Computing* 2019. doi: 10.1007/s10915-019-00976-5
33. Negri F. redbKIT. <http://redbkit.github.io/redbKIT/>; 2016. Version 2.2.
34. Haasdonk B. *RBmatlab*. 2016.
35. Haasdonk B. Reduced basis methods for parametrized PDEs—A tutorial introduction for stationary and instationary problems. *Reduced Order Modelling. Luminy Book series* 2014.
36. Negri F, Manzoni A, Amsallem D. Efficient model reduction of parametrized systems by matrix discrete empirical interpolation. *Journal of Computational Physics* 2015; 303: 431–454.
37. Kasolis F, Wadbro E, Berggren M. Fixed-mesh curvature-parameterized shape optimization of an acoustic horn. *Structural and Multidisciplinary Optimization* 2012; 46(5): 727–738.
38. Buhmann MD. *Radial basis functions: theory and implementations*. 12. Cambridge university press . 2003.
39. Bängtsson E, Noreland D, Berggren M. Shape optimization of an acoustic horn. *Computer methods in applied mechanics and engineering* 2003; 192(11-12): 1533–1571.
40. Manzoni A, Quarteroni A, Rozza G. Model reduction techniques for fast blood flow simulation in parametrized geometries. *International journal for numerical methods in biomedical engineering* 2012; 28(6-7): 604–625.
41. Quarteroni A, Manzoni A, Negri F. *Reduced basis methods for partial differential equations: an introduction*. 92. Springer . 2015.
42. Benaceur A, Ehrlacher V, Ern A, Meunier S. A progressive reduced basis/empirical interpolation method for nonlinear parabolic problems. *SIAM Journal on Scientific Computing* 2018; 40(5): A2930–A2955.
43. Chen Y, Hesthaven JS, Maday Y, Rodríguez J, Zhu X. Certified reduced basis method for electromagnetic scattering and radar cross section estimation. *Computer methods in applied mechanics and engineering* 2012; 233: 92–108.

